EMJ MS
EUROPEAN MULTIDISCIPLINARY JOURNAL OF MODERN SCIENCE
https://emjms.academicjournal.io
Special Issue: Use of Modern Innovation on Integrated Research

Study a Spalart-Allmares Turbulence Model for the Calculation of a Centrifugal Separator

Murodil Erkinjon Ugli Madaliev, Giyosiddin Ilhomiddinovich Mamatisayev, Doniyorjon Ravshanjon ugli Srojidinov
1Ferghana Polytechnic Institute, Ferghana, 86 Ferghana str., 150107, Uzbekistan

Abstract: A study of SA models of turbulence as applied to the calculation of swirling flows inside a separator has been carried out. The paper compared two approaches using vorticity and stream function to eliminate pressure and a semi-implicit pressure-related SIMPLE method for solving Reynolds-averaged Navier-Stokes equations. For the numerical solution of both approaches, the implicit upstream method was used.

Keywords: Navier–Stokes equations, control volume method, SIMPLE method, SA model.

INTRODUCTION

In modern technological processes, swirling flows of gases and liquids are often encountered [1]. Swirling currents are formed behind the wheels of hydraulic turbines of HT [2], in the wake of aircraft and propellers, as well as wind turbines, etc. [3]. Cyclones, separators, vortex flowmeters - all these devices use swirling of the flow of the working medium. The useful properties of swirling flows are widely used in thermal power engineering, for example, with the help of it they achieve flame stabilization in burners. However, swirling flows have not only positive features. In strongly swirling flows, the formation of unsteady structures, such as a precessing vortex core (PVC), often occurs. The low frequencies of the precession of the vortex core, which is formed, for example, behind the wheel of a hydro turbine of a hydroelectric power station, can lead to resonance with the natural frequencies of the hydroelectric unit, which in turn will entail strong vibrations that pose a serious danger to the entire structure of the hydroelectric power station. The formation of PVCs in vortex combustion chambers can cause thermoacoustic resonance [4], which also results in strong vibrations and noise. In addition, it was found that the PVC can affect the efficiency of the vortex devices [5]. Large-scale pulsations caused by vortex precession can damage structures and reduce equipment reliability. Despite many years of research into this phenomenon, at the moment there is not enough information to build a theory of PVC and, accordingly, to develop effective methods for controlling this phenomenon. Thus, for engineering calculations, turbulence models are required that accurately describe the averaged fields and large-scale pulsations of swirling flows. Widely used in engineering calculations $k-\varepsilon$ and $k-\omega$ turbulence models do not describe such flows well. To improve the adequacy of modeling turbulent swirling flows, they try to modify the existing RANS models (Reynolds-Averaged Navier-Stokes Equations - Reynolds-averaged Navier-Stokes equations) of turbulence. In [6], Spalart and Allmaras proposed the Spalart-Allmaras model. New model dubbed SA.

PHYSICAL AND MATHEMATICAL STATEMENT OF THE PROBLEM.

It is known that swirling flows are characterized by a strong curvature of the streamlines, the appearance of recirculation zones, the location and size of which largely depend on the intensity of the twist and the configuration of the boundaries. In addition, such flows are turbulent. Therefore, their study requires the involvement of efficient turbulence models. Quite effective turbulence models have recently appeared

In this paper, we consider a two-dimensional axisymmetric turbulent flow in an air centrifugal separator, which is an important link in the separation and classification of particles, obtaining powders of the required quality. The efficiency of ongoing processes for separating powders into coarse and fine fractions will depend on how the flow structure is organized within the working area. The purpose of this numerical study is to elucidate the nature of the hydrodynamics of a swirling flow for different geometries. The scheme of the calculated area is shown in fig. 1.

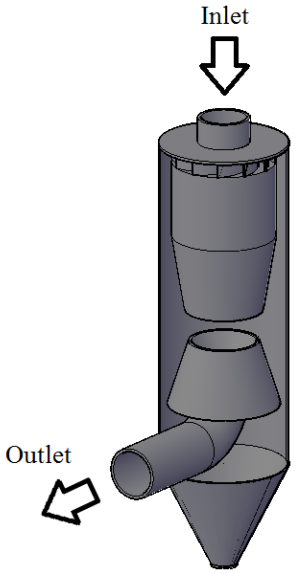

Fig. 1 Scheme of calculated air centrifugal separator.

Centrifugal air separator works as follows. The feed material, together with the primary air, is fed through a branch pipe into the upper part of the separator. With the help of controlled shovels, the air flow is given a rotational motion. Under the action of the centrifugal force of inertia, the particles move towards the outer cylindrical wall of the separator housing and enter the classification zone located between the cones and the wall (see Fig. 1). Large particles, due to their greater mass, under the action of centrifugal force, accumulate near the inner wall of the separator housing and, by inertia, enter the separator hopper. And small particles are carried away by air and are taken out of the separator through the outlet pipe. Thus, the initial material is divided into two fractions [12].

It is easy to understand that the efficiency of such a separator strongly depends on its geometry. Therefore, to search for the optimal geometric parameters, the problem arises of modeling the kinematics of particles inside the facility. It is clear that the kinematics of the particles depends on the dynamics of the air flow. Therefore, two problems arise here: 1) to study the dynamics of the air flow; 2) based on the obtained hydrodynamic parameters of the air flow, investigate the trajectories of the separated particles.

In practice, the bulk density of dust in separators can reach 50 $г/м^3$. This value is

significantly less than the density of incompressible air (2.3 $кг/м^3$). Therefore, in many works, the influence of the solid phase on the air dynamics is neglected. Modeling of three-dimensional gas flows is associated with well-known practical difficulties: the use of staggered grids in a continuous calculation area, slow convergence of the numerical solution algorithm, and rather complicated implementation of the calculation algorithm. The solution of the turbulent problem also requires thickening the computational stack in regions with large gradients of the desired variables, in particular, near solid walls. All these problems significantly complicate the solution of the problem in the area under consideration.

For the numerical study of the problem posed, the system of equations averaged by Reynolds of the Navier-Stokes equations in a cylindrical coordinate system is used [7]:

$$\begin{cases} \frac{\partial U}{\partial z}+\frac{\partial rV}{r\partial r}=0, \\ \frac{\partial U}{\partial t}+U\frac{\partial U}{\partial z}+V\frac{\partial U}{\partial r}+\frac{1}{\rho}\frac{\partial P}{\partial z}=\frac{1}{r}\frac{\partial}{\partial r}\left[r\nu_{eff}\frac{\partial U}{\partial r}\right], \\ \frac{\partial V}{\partial t}+U\frac{\partial V}{\partial z}+V\frac{\partial V}{\partial r}-\frac{G^2}{r^3}+\frac{1}{\rho}\frac{\partial P}{\partial r}=\frac{1}{r}\frac{\partial}{\partial r}\left[r\nu_{eff}\frac{\partial V}{\partial r}\right]-\frac{\mu}{r^2}V, \\ \frac{\partial G}{\partial t}+U\frac{\partial G}{\partial z}+V\frac{\partial G}{\partial r}=\frac{\partial}{r\partial r}\left(\nu_{eff}\frac{\partial G}{\partial r}\right)-\frac{\partial}{r^2\partial r}\left(2\nu_{eff}G\right)+\frac{2\nu_{eff}G}{r^3}; \\ G=W\times r;\ \ \nu_{eff}=\nu+\nu_t \end{cases} \quad (1)$$

here v, v_t - molecular and turbulent viscosity, U,V,W- dimensionless averaged velocity vectors; r,z- dimensionless coordinates; The initial and boundary conditions for the system of equations (1) are set in the standard way [8].

At $z=0: U=U_0,\ V=0, W=W_0.$

On the walls: $U=V=W=0.$

on axle $r=0$: $\frac{\partial\Phi}{\partial r}=0$ for $\Phi=U$ и $W,V=0.$

The main section was disassembled into 4 sections shown in Fig. 2.

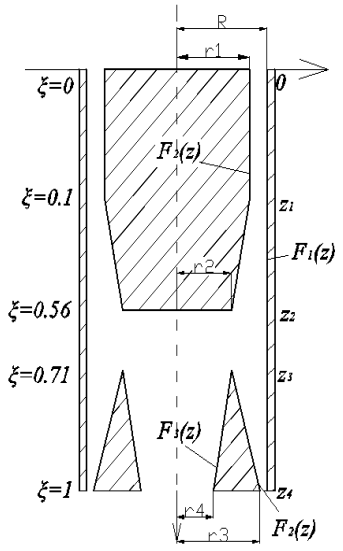

Fig. 2. Flow region in the separator in dimensionless coordinates.

where R is the large radius of the annular channel, therefore, the surface of the cone corresponds to $\eta = 1$; r_1- radius of the inner cylinder of the first section, r_3, r_4- radius of inner cylinder rub and fourth plots.

To calculate equation (1) of complex figures, we change the coordinate system. We write system (1) in the von Mises variables [9] *(z, r)* on the -*(ξ, η),* where *ξ=z/L*. In new variables, derivatives are determined by the well-known formula:

$$\frac{\partial}{\partial z} = \frac{\partial \xi}{\partial z}\frac{\partial}{\partial \xi} + \frac{\partial \eta}{\partial z}\frac{\partial}{\partial \eta} = \frac{\partial}{\partial \xi} + \eta'\frac{\partial}{\partial \eta}, \quad \frac{\partial}{\partial r} = \frac{\partial \xi}{\partial r}\frac{\partial}{\partial \xi} + \frac{\partial \eta}{\partial r}\frac{\partial}{\partial \eta} = F(z)\frac{\partial}{\partial \eta}.$$

First plot $(0 < z < z_2)$:

$$\eta = \frac{\eta_0 F_1(z) - F_2(z)}{F_1(z) - F_2(z)} + \frac{(1-\eta_0)r}{F_1(z) - F_2(z)}, \eta' = \frac{(\eta_0 F_1'(z) - F_2'(z))}{(F_1(z) - F_2(z))} - \frac{(\eta_0 F_1(z) - F_2(z))(F_1'(z) - F_2'(z))}{(F_1(z) - F_2(z))^2} - \frac{r(1-\eta_0)(F_1'(z) - F_2'(z))}{(F_1(z) - F_2(z))^2},$$

$$\eta'' = -\frac{(F_1'(z) - F_2'(z))(\eta_0 F_1'(z) - F_2'(z))}{(F_1(z) - F_2(z))^2} - \frac{(\eta_0 F_1'(z) - F_2'(z))(F_1'(z) - F_2'(z))(F_1(z) - F_2(z)) - 2(\eta_0 F_1(z) - F_2(z))(F_1'(z) - F_2'(z))^2}{(F_1(z) - F_2(z))^3} +$$

$$+ \frac{2r(1-\eta_0)(F_1'(z) - F_2'(z))^2}{(F_1(z) - F_2(z))^3} \; npu \; F_1(z) = R, \qquad F_2(z) = r_2.$$

Second plot $(z_2 < z < z_3)$:

$$\eta = \frac{r - F_2(z)}{(F_1(z) - F_2(z))}, \eta' = -\frac{F_2'(z)}{f_1 - f_2} - \frac{(r - F_2(z))(F_1'(z) - F_2'(z))}{(F_1(z) - F_2(z))^2},$$

$$\eta'' = \frac{F_2'(z)(F_1'(z) - F_2'(z))}{(F_1(z) - F_2(z))^2} - \left(\frac{F_2'(z)(F_1'(z) - F_2'(z))(F_1(z) - F_2(z)) - 2(F_1'(z) - F_2'(z))^2 (r - F_2(z))}{(F_1(z) - F_2(z))^3} \right),$$

$$npu \;\; F_1(z) = R, \qquad F_2(z) = 0.$$

Third plot $(z_3 < z < z_4,\ \eta < \eta_0)$:

$$\eta = \eta_0 \frac{r}{F_3(z)}, \eta' = -\eta_0 \frac{r}{F_3^2(z)}, \eta'' = \eta_0 \frac{2r * F_3'(z)}{F_3^3(z)} \; npu \; F_3(z) = r_2, \qquad F_2(z) = 0.$$

Fourth section $(z_3 < z < z_4,\ \eta > \eta_0)$:

$$\eta = \frac{\eta_0 F_1(z) - F_2(z)}{F_1(z) - F_2(z)} + \frac{(1-\eta_0)r}{F_1(z) - F_2(z)}, \; \eta' = -\frac{F_2'(z)}{f_1 - f_2} - \frac{(r - F_2(z))(F_1'(z) - F_2'(z))}{(F_1(z) - F_2(z))^2},$$

$$\eta'' = \frac{F_2'(z)(F_1'(z) - F_2'(z))}{(F_1(z) - F_2(z))^2} - \left(\frac{F_2'(z)(F_1'(z) - F_2'(z))(F_1(z) - F_2(z)) - 2(F_1'(z) - F_2'(z))^2 (r - F_2(z))}{(F_1(z) - F_2(z))^3} \right)$$

$$npu \; F_1(z) = R, \qquad F_2(z) = r_4.$$

Here $F_1(z)$- outer cylinder function, $F_2(z)$, $F_3(z)$- inner cylinder and cone functions; $\eta_0 = 0.6\eta$

In the new variables, the system of equations (1) takes the form

$$\begin{cases} \frac{\partial U}{\partial \xi}+\eta'\frac{\partial U}{\partial \eta}+F(z)\frac{\partial rV}{r\partial \eta}=0, \\ \frac{\partial U}{\partial t}+U\frac{\partial U}{\partial \xi}+U\eta'\frac{\partial U}{\partial \eta}+V\times F(z)\frac{\partial U}{\partial \eta}+\frac{\partial P}{\partial \xi}+\eta'\frac{\partial P}{\partial \eta}=\frac{F(z)}{r}\frac{\partial}{\partial \eta}\left[r\nu_{eff}F(z)\frac{\partial U}{\partial \eta}\right], \\ \frac{\partial V}{\partial t}+U\frac{\partial V}{\partial \xi}+U\eta'\frac{\partial V}{\partial \eta}+V\times F(z)\frac{\partial V}{\partial \eta}-\frac{G^2}{r^3}+F(z)\frac{\partial P}{\partial \eta}=\frac{F(z)}{r}\frac{\partial}{\partial \eta}\left[r\nu_{eff}F(z)\frac{\partial V}{\partial \eta}\right]-\frac{\nu_{eff}}{r^2}V, \\ \frac{\partial G}{\partial t}+U\frac{\partial G}{\partial \xi}+U\eta'\frac{\partial G}{\partial \eta}+V\times F(z)\frac{\partial G}{\partial \eta}=\frac{F(z)}{r}\frac{\partial}{\partial \eta}\left(\nu_{eff}F(z)\frac{\partial G}{\partial \eta}\right)-\frac{F(z)}{r^2}\frac{\partial}{\partial \eta}(2\nu_{eff}G)+\frac{2\nu_{eff}G}{r^3}, \\ \nu_{eff}=\nu+\nu_t \end{cases} \quad (2)$$

On the system equation (2) $F(z)$ - a function that depends on the calculated area $\eta_0=0.6\eta$

$$F(z)=\begin{cases} \frac{(1-\eta_0)}{F_1(z)-F_2(z)}npu(0<z<z_2), \\ \frac{1}{F_1(z)-F_2(z)}npu(z_2<z<z_3), \\ \eta_0\frac{1}{F_3}npu(z_3<z<z_4,\eta<\eta_0), \\ \frac{(1-\eta_0)}{F_1(z)-F_2(z)}npu(z_3<z<z_4,\eta>\eta_0). \end{cases}$$

The Reynolds-averaged equations of the Navier-Stokes equations were closed using the turbulence model: Spalart-Allmaras.

Spalart-Allmaras models [6]. This model belongs to the class of one-parameter turbulence models. Here there is only one additional equation for calculating the kinematic coefficient of eddy viscosity

$$\frac{\partial \rho\tilde{\nu}}{\partial t}+\nabla(\rho\tilde{\nu}U)=\rho(P_\nu-D_\nu)+\frac{1}{\sigma_\nu}\nabla[(\nu+\nu_t)\nabla\tilde{\nu}]+\frac{C_{b2}}{\sigma_\nu}\rho(\nabla\tilde{\nu})^2-\frac{1}{\sigma_\nu\rho}(\mu+\rho\tilde{\nu})\nabla\rho\nabla\tilde{\nu}. \quad (3)$$

Turbulent eddy viscosity is calculated from: $\nu_t=\tilde{\nu}f_{v1}$

Initial and boundary conditions. The parameters of the undisturbed flow in the entire computational domain were set as the initial conditions. At the outer boundary, non-reflective boundary conditions were applied. On the surface of a solid body, the no-slip condition was set. In the SA turbulence model, the value of the working variable on the body was set to zero $v_t = 0$, at the entrance border $v_t = 3v$, on the day off - the Neumann condition was set.

SOLUTION METHODS

Using vorticity and stream function [13]

To facilitate the numerical implementation in system (1), a partial parabolization was carried out, i.e. terms with derivatives with respect to z were neglected on the right-hand sides. We introduce the stream function ψ, for which the continuity condition is satisfied:

$$V=-\frac{1}{r}\frac{\partial\psi}{\partial z},\ U=\frac{1}{r}\frac{\partial\psi}{\partial r}. \quad (4)$$

We also introduce vorticity ζ

$$\zeta = \frac{\partial U}{\partial r} - \frac{\partial V}{\partial z}. \qquad (5)$$

Further, from the first two equations of system (1), we eliminate the pressure and, substituting expressions (4) into (5), we obtain a system with respect to new variables.

$$\begin{cases} \dfrac{\partial \zeta}{\partial t} + U\dfrac{1}{L}\dfrac{\partial \zeta}{\partial \xi} + U\eta'\dfrac{\partial \zeta}{\partial \eta} + F(z)V\dfrac{\partial \zeta}{\partial \eta} - \zeta\dfrac{V}{r} + \dfrac{1}{r^2}\dfrac{1}{L}\dfrac{\partial G^2}{\partial \xi} + \dfrac{\eta'}{r^2}\dfrac{\partial G^2}{\partial \eta} = -\dfrac{F(z)}{r^2}\dfrac{\partial\left(r(\nu_{eff})\zeta\right)}{\partial \eta} + \dfrac{F(z)^2}{r}\dfrac{\partial^2\left(r(\nu_{eff})\zeta\right)}{\partial \eta^2}, \\ \dfrac{\partial G}{\partial t} + \dfrac{U}{L}\dfrac{\partial G}{\partial \xi} + U\eta'\dfrac{\partial G}{\partial \eta} + F(z)V\dfrac{\partial G}{\partial \eta} = F(z)\dfrac{\partial}{\partial \eta}\left((\nu_{eff})\left(F(z)\dfrac{\partial G}{\partial \eta} - \dfrac{G}{r}\right)\right) - \dfrac{\mu}{r^2}G, \\ \dfrac{F(z)^2}{r}\dfrac{\partial^2 \psi}{\partial \eta^2} - \dfrac{F(z)}{r^2}\dfrac{\partial \psi}{\partial \eta} + \dfrac{1}{rL^2}\dfrac{\partial^2 \psi}{\partial \xi^2} + 2\dfrac{\eta'}{rL}\dfrac{\partial^2 \psi}{\partial \xi \partial \eta} + (\eta')^2\dfrac{\partial^2 \psi}{r\partial \eta^2} + \eta''\dfrac{\partial \psi}{r\partial \eta} = \zeta, \\ \psi = -\dfrac{1}{L}\dfrac{\partial V}{\partial \xi} + \eta'\dfrac{\partial V}{\partial \eta}, \quad \psi = F(z)\dfrac{\partial U}{\partial \eta}, \\ \dfrac{\partial \tilde{\nu}}{\partial t} + U\dfrac{\partial \tilde{\nu}}{\partial \xi} + U\eta'\dfrac{\partial \tilde{\nu}}{\partial \eta} + F(z)V\dfrac{\partial \tilde{\nu}}{\partial \eta} = (P\nu - D\nu) + \dfrac{F(z)}{r\sigma_\nu}\dfrac{\partial}{\partial \eta}\left[r(\nu + \tilde{\nu})F(z)\dfrac{\partial \tilde{\nu}}{\partial \eta}\right] + \dfrac{C_{b2}}{\sigma_\nu}\left(F(z)\dfrac{\partial \tilde{\nu}}{\partial \eta}\right)^2. \end{cases} \qquad (6)$$

Thus, the new variables allow us to bring all the equations of the system to a parabolic form, and this system can be written in vector form

$$\frac{\partial \Phi}{\partial t} + U\frac{\partial \Phi}{\partial \xi} + U\eta'\frac{\partial \Phi}{\partial \eta} + V\eta\frac{\partial \Phi}{\partial \eta} = F(z)^2\frac{\partial}{\partial \eta}\left(a^{(\Phi)}\frac{\partial \Phi}{\partial \eta}\right) + \Pi^{(\Phi)} \qquad (7)$$

For the numerical implementation of ζ, G and ν in Eqs. (7), the implicit scheme was used

$$\Phi = \begin{bmatrix} \zeta \\ G \\ \tilde{\nu} \end{bmatrix}, \ \Pi^{(\Phi)} = \begin{bmatrix} F(z)V\dfrac{\partial \zeta}{\partial \eta} - \zeta\dfrac{V}{r} + \dfrac{1}{Lr^2}\dfrac{\partial G^2}{\partial \xi} + \dfrac{\eta'}{r^2}\dfrac{\partial G^2}{\partial \eta} \\ 0 \\ (P\nu - D\nu) + \dfrac{C_{b2}}{\sigma_\nu}\left(F(z)\dfrac{\partial \tilde{\nu}}{\partial \eta}\right)^2 \end{bmatrix}, \ a^{(\Phi)} = \begin{bmatrix} r(\nu_{eff}) \\ 1 \\ r(\nu + \tilde{\nu})F(z) \end{bmatrix}.$$

The upstream circuit has the form

$$U = U_{i,j}^n, \ V = \left(U_{i,j}^n\eta' + V_{i,j}^n F(z)\right),$$

$$\frac{\Phi_{i,j}^{n+1} - \Phi_{i,j}^n}{\Delta t} + \frac{0.5\left(U_{i,j} + |U_{i,j}|\right)}{L}\frac{\Phi_{i,j}^n - \Phi_{i-1,j}^n}{\Delta \xi} + \frac{0.5\left(U_{i,j} - |U_{i,j}|\right)}{L}\frac{\Phi_{i+1,j}^n - \Phi_{i,j}^n}{\Delta \xi} + 0.5\eta'\left(U_{i,j} + |U_{i,j}|\right)\frac{\Phi_{i,j}^n - \Phi_{i,j-1}^n}{\Delta \eta} +$$

$$+ 0.5\eta'\left(U_{i,j} - |U_{i,j}|\right)\frac{\Phi_{i,j+1}^n - \Phi_{i,j}^n}{\Delta \eta} + 0.5F(z)\left(V_{i,j} + |V_{i,j}|\right)\frac{\Phi_{i,j}^n - \Phi_{i,j-1}^n}{\Delta \eta} + 0.5F(z)\left(V_{i,j} - |V_{i,j}|\right)\frac{\Phi_{i,j+1}^n - \Phi_{i,j}^n}{\Delta \eta} =$$

$$= F(z)\frac{\Phi_{i,j+1}^{n+1}(a_{i,j+1}^{(\Phi)} + a_{i,j}^{(\Phi)}) - \Phi_{i,j}^{n+1}(a_{i,j+1}^{(\Phi)} + 2a_{i,j}^{(\Phi)} + a_{i,j-1}^{(\Phi)}) + \Phi_{i,j-1}^{n+1}(a_{i,j}^{(\Phi)} + a_{i,j-1}^{(\Phi)})}{2r_j\Delta\eta^2} + \Pi^{(\Phi)}.$$

(8)

It is absolutely stable and the unknowns on the new layer were found by the sweep method. The integration steps were $\Delta\xi = 0.05, \Delta\eta = 0.02.$ The number of calculated points in the transverse direction was 50, in the longitudinal direction 100. The Poisson equation for the stream function was also approximated by the central difference, and the upper relaxation iteration method was used to resolve it.

$$\frac{\psi^k{}_{i+1,j} - 2\psi^{k+1}{}_{i,j} + \psi^k{}_{i-1,j}}{\Delta\xi^2} + \frac{\psi^k{}_{i,j+1} - \psi^k{}_{i,j-1}}{2\Delta\eta} + \frac{\psi^k{}_{i+1,j+1} - \psi^k{}_{i-1,j+1} + \psi^k{}_{i+1,j-1} - \psi^k{}_{i-1,j-1}}{2\Delta\xi\Delta\eta} + \frac{\psi^k{}_{i,j+1} - 2\psi^{k+1}{}_{i,j} + \psi^k{}_{i,j-1}}{\Delta\eta^2} = r_j\zeta^k{}_{i,j}.$$

(9)

Semi-Implicit Method for Pressure-Binding SIMPLE

The numerical solution of the presented system of equations was carried out in the physical variables velocity–pressure by physically splitting the velocity and pressure fields [10]. The numerical solution of the transport equation is carried out on a hybrid, checkerboard difference grid using the control volume method. According to this method, the solution of the Reynolds equations written in the cylindrical coordinate of new variables includes two stages:

$$\begin{cases} \frac{\tilde{U}-U^n}{\Delta t}+U^n\frac{\partial U^n}{\partial \xi}+U^n\eta'\frac{\partial U^n}{\partial \eta}+V^n\times F(z)\frac{\partial U^n}{\partial \eta}+\frac{\partial P}{\partial \xi}+\eta'\frac{\partial P}{\partial \eta}=\frac{F(z)}{r}\frac{\partial}{\partial \eta}\left[r\nu_{eff}F(z)\frac{\partial \tilde{U}}{\partial \eta}\right], \\ \frac{\tilde{V}-V^n}{\Delta t}+U^n\frac{\partial V^n}{\partial \xi}+U^n\eta'\frac{\partial V^n}{\partial \eta}+V^n\times F(z)\frac{\partial V^n}{\partial \eta}-\frac{G^2}{r^3}+F(z)\frac{\partial P}{\partial \eta}=\frac{F(z)}{r}\frac{\partial}{\partial \eta}\left[r\nu_{eff}F(z)\frac{\partial \tilde{V}}{\partial \eta}\right]-\frac{\nu_{eff}}{r^2}\tilde{V}, \\ \frac{\tilde{G}-G^n}{\Delta t}+U^n\frac{\partial G^n}{\partial \xi}+U^n\eta'\frac{\partial G^n}{\partial \eta}+V^n\times F(z)\frac{\partial G^n}{\partial \eta}=\frac{F(z)}{r}\frac{\partial}{\partial \eta}\left(r\nu_{eff}F(z)\frac{\partial \tilde{G}}{\partial \eta}\right)-\frac{F(z)}{r^2}\frac{\partial}{\partial \eta}\left(2\nu_{eff}\tilde{G}\right)+\frac{2\nu_{eff}}{r^2}\tilde{G}, \\ \frac{\partial \tilde{\nu}}{\partial t}+U\frac{\partial \tilde{\nu}}{\partial \xi}+U\eta'\frac{\partial \tilde{\nu}}{\partial \eta}+F(z)V\frac{\partial \tilde{\nu}}{\partial \eta}=(P\nu-D\nu)+\frac{F(z)}{r\sigma_\nu}\frac{\partial}{\partial \eta}\left[r(\nu_{eff})F(z)\frac{\partial \tilde{\nu}}{\partial \eta}\right]+\frac{C_{b2}}{\sigma_\nu}\left(F(z)\frac{\partial \tilde{\nu}}{\partial \eta}\right)^2, \\ \nu_{eff}=\frac{1}{\mathrm{Re}}+\nu_t \end{cases} \quad (10)$$

$$\begin{cases} U^{n+1}=\tilde{U}-\Delta t\frac{\partial \delta p}{\partial z} \\ V^{n+1}=\tilde{V}-\Delta t\frac{\partial \delta p}{\partial r} \end{cases} \quad (11)$$

Equation (10) is a system of RANS equations written in the cylindrical coordinate of new variables. The superscript "$\tilde{U}$ "denotes an intermediate grid function for the velocity vector; $\delta p = p^{n+1} - p^n$ pressure correction. Multiplying equation (11) by the gradient and taking into account the solenoidality of the velocity vector at the (n + 1) -th time layer, we obtain the Poisson equation for determining the correction to pressure:

$$\Delta t\left(\frac{\partial^2 \delta p}{\partial z^2}+\frac{\partial^2 \delta p}{\partial r^2}+\frac{\partial \delta p}{r\partial r}\right)=\frac{\partial U^n}{\partial z}+\frac{\partial rV^n}{r\partial r}; \quad (12)$$

Equation (12) of new variables has the form:

$$\Delta t\left(\frac{\partial^2 \delta p}{\partial \xi^2}+2\eta'\frac{\partial^2 \delta p}{\partial \xi\partial \eta}+(\eta')^2\frac{\partial^2 \delta p}{\partial \eta^2}+\eta''\frac{\partial \delta p}{\partial \eta}+A^2\frac{\partial^2 \delta p}{\partial \eta^2}+A\frac{\partial \delta p}{r\partial \eta}\right)=\frac{\partial U^n}{\partial \xi}+\eta'\frac{\partial U^n}{\partial \eta}+A\frac{\partial rV^n}{r\partial \eta}. \quad (13)$$

The solution of the stationary problem is carried out by the method of establishment in time, therefore, dependence (13) is written in the form of a non-stationary differential equation

$$\frac{\partial \delta p}{\partial t_0}-\Delta t\left(\frac{\partial^2 \delta p}{\partial \xi^2}+2\eta'\frac{\partial^2 \delta p}{\partial \xi\partial \eta}+(\eta')^2\frac{\partial^2 \delta p}{\partial \eta^2}+\eta''\frac{\partial \delta p}{\partial \eta}+A^2\frac{\partial^2 \delta p}{\partial \eta^2}+A\frac{\partial \delta p}{r\partial \eta}\right)=\frac{\partial U^n}{\partial \xi}+\eta'\frac{\partial U^n}{\partial \eta}+A\frac{\partial rV^n}{r\partial \eta}. \quad (14)$$

where the fictitious time t_0 is the iterative parameter. When solving equation (14) for the time step, we can write $\Delta t_0 = a_1 \Delta t$, while the value of the constant a_1, as a rule, is less than unity and is chosen from the condition of rapid convergence of the numerical process. The Neumann condition is used as the boundary condition for the pressure correction, which is satisfied if the exact value of $\tilde{U}$ is used for U^{n+1} at the boundary [11-23]:

For the numerical solution of the transport equation of system (10), a finite-difference scheme against the flow was used, which has a second-order accuracy, i.e. $O(\Delta t, \Delta\xi^2, \Delta\eta^2)$.

$$\begin{cases} \frac{\tilde{U}-U^n}{\Delta t}+U^n\frac{\partial U^n}{\partial\xi}+U^n\eta'\frac{\partial U^n}{\partial\eta}+V^n\times F(z)\frac{\partial U^n}{\partial\eta}+\frac{\partial P}{\partial\xi}+\eta'\frac{\partial P}{\partial\eta}=\frac{F(z)}{r}\frac{\partial}{\partial\eta}\left[r\nu_{eff}F(z)\frac{\partial\tilde{U}}{\partial\eta}\right], \\ \frac{\tilde{V}-V^n}{\Delta t}+U^n\frac{\partial V^n}{\partial\xi}+U^n\eta'\frac{\partial V^n}{\partial\eta}+V^n\times F(z)\frac{\partial V^n}{\partial\eta}-\frac{G^2}{r^3}+F(z)\frac{\partial P}{\partial\eta}=\frac{F(z)}{r}\frac{\partial}{\partial\eta}\left[r\nu_{eff}F(z)\frac{\partial\tilde{V}}{\partial\eta}\right]-\frac{\nu_{eff}}{r^2}\tilde{V}, \\ \frac{\tilde{G}-G^n}{\Delta t}+U^n\frac{\partial G^n}{\partial\xi}+U^n\eta'\frac{\partial G^n}{\partial\eta}+V^n\times F(z)\frac{\partial G^n}{\partial\eta}=\frac{F(z)}{r}\frac{\partial}{\partial\eta}\left(r\nu_{eff}F(z)\frac{\partial\tilde{G}}{\partial\eta}\right)-\frac{F(z)}{r^2}\frac{\partial}{\partial\eta}\left(2\nu_{eff}\tilde{G}\right)+\frac{2\nu_{eff}}{r^2}\tilde{G}, \\ \frac{\partial\tilde{\nu}}{\partial t}+U\frac{\partial\tilde{\nu}}{\partial\xi}+U\eta'\frac{\partial\tilde{\nu}}{\partial\eta}+F(z)V\frac{\partial\tilde{\nu}}{\partial\eta}=(Pv-Dv)+\frac{F(z)}{r\sigma_v}\frac{\partial}{\partial\eta}\left[r(\nu_{eff})F(z)\frac{\partial\tilde{\nu}}{\partial\eta}\right]+\frac{C_{b2}}{\sigma_v}\left(F(z)\frac{\partial\tilde{\nu}}{\partial\eta}\right)^2, \\ \nu_{eff}=\frac{1}{\mathrm{Re}}+\nu_t \end{cases} \quad (15)$$

$$\Phi=\begin{bmatrix}U\\V\\G\\\tilde{\nu}\end{bmatrix},\ \Pi^{(\Phi)}=\begin{bmatrix}-\left(\frac{\partial P}{\partial\xi}+\eta'\frac{\partial P}{\partial\eta}\right)\\ \frac{G^2}{r^3}-F(z)\frac{\partial P}{\partial\eta}-\frac{\nu_{eff}}{r^2}\tilde{V}\\ -\frac{F(z)}{r^2}\frac{\partial}{\partial\eta}\left(2\nu_{eff}\tilde{G}\right)+\frac{2\nu_{eff}}{r^2}\tilde{G},\\ (Pv-Dv)+\frac{C_{b2}}{\sigma_v}\left(F(z)\frac{\partial\tilde{\nu}}{\partial\eta}\right)^2\end{bmatrix},\ a^{(\Phi)}=\begin{bmatrix}r\nu_{eff}F(z)\\ r\nu_{eff}F(z)\\ r\nu_{eff}F(z)\\ r(v+\tilde{\nu})F(z)\end{bmatrix}.$$

The upstream circuit has the form

$$U_{i,j}=U^n_{i,j},\quad V_{i,j}=\left(U^n_{i,j}\eta'+V^n_{i,j}F(z)\right),$$

$$\frac{\Phi^{n+1}_{i,j}-\Phi^n_{i,j}}{\Delta t}+\frac{0.5\left(U_{i,j}+\left|U_{i,j}\right|\right)}{L}\frac{\Phi^n_{i,j}-\Phi^n_{i-1,j}}{\Delta\xi}+\frac{0.5\left(U_{i,j}-\left|U_{i,j}\right|\right)}{L}\frac{\Phi^n_{i+1,j}-\Phi^n_{i,j}}{\Delta\xi}+0.5\eta'\left(U_{i,j}+\left|U_{i,j}\right|\right)\frac{\Phi^n_{i,j}-\Phi^n_{i,j-1}}{\Delta\eta}+$$

$$0.5\eta'\left(U_{i,j}-\left|U_{i,j}\right|\right)\frac{\Phi^n_{i,j+1}-\Phi^n_{i,j}}{\Delta\eta}+0.5F(z)\left(V_{i,j}+\left|V_{i,j}\right|\right)\frac{\Phi^n_{i,j}-\Phi^n_{i,j-1}}{\Delta\eta}+0.5F(z)\left(V_{i,j}-\left|V_{i,j}\right|\right)\frac{\Phi^n_{i,j+1}-\Phi^n_{i,j}}{\Delta\eta}=$$

$$=F(z)\frac{\Phi^{n+1}_{i,j+1}(a^{(\Phi)}_{i,j+1}+a^{(\Phi)}_{i,j})-\Phi^{n+1}_{i,j}(a^{(\Phi)}_{i,j+1}+2a^{(\Phi)}_{i,j}+a^{(\Phi)}_{i,j-1})+\Phi^{n+1}_{i,j-1}(a^{(\Phi)}_{i,j}+a^{(\Phi)}_{i,j-1})}{2r_j\Delta\eta^2}+\Pi^{(\Phi)}.$$

(16)

The pressure correction equation in system (14) has an elliptical form. For the numerical solution of such equations, the relaxation method in the direction of η and the sweep in ξ are effective and quite simple.

$$\frac{\delta p^{n+1}_{i,j}-\delta p^n_{i,j}}{\Delta t_0}-\left(\frac{\delta p^n_{i+1,j}-2\delta p^{n+1}_{i,j}+\delta p^n_{i-1,j}}{\Delta\xi^2}+\eta'\frac{\delta p^n_{i+1,j+1}-\delta p^n_{i+1,j-1}-\delta p^n_{i-1,j+1}+\delta p^n_{i-1,j-1}}{2\Delta\xi\Delta\eta}\right)-$$

$$-\left(\left((\eta')^2+F(z)^2\right)\frac{\delta p^{n+1}_{i,j+1}-2\delta p^{n+1}_{i,j}+\delta p^{n+1}_{i,j-1}}{\Delta\eta^2}+\left(\eta''+\frac{F(z)}{r_j}\right)\frac{\delta p^{n+1}_{i,j+1}-\delta p^{n+1}_{i,j-1}}{2\Delta\eta}\right)= \quad (17)$$

$$=\frac{1}{\Delta t}\left(\frac{U^n_{i,j}-U^n_{i-1,j}}{\Delta\xi}+\eta'\frac{U^n_{i,j}-U^n_{i,j-1}}{\Delta\eta}+F(z)\frac{V^n_{i,j}r_j-V^n_{i,j-1}r_{j-1}}{r_j\Delta\eta}\right).$$

Thus, first the system of equations (10) is solved by the establishment method, then equation (12) and in accordance with (11) the velocity vector on the (n + 1) -th time layer and pressure are determined. $\delta p^{n+1}=p^n+\delta p$

The Pascal ABC program was used to calculate the problem.

THE DISCUSSION OF THE RESULTS

On fig. 3 illustrates the profiles of air velocities in the section $\xi = 0.65$. Here $U/Uref, V/Uref, W/Uref$ - dimensionless speeds. Here $Uref = U_0, Wref/Uref = 1$.

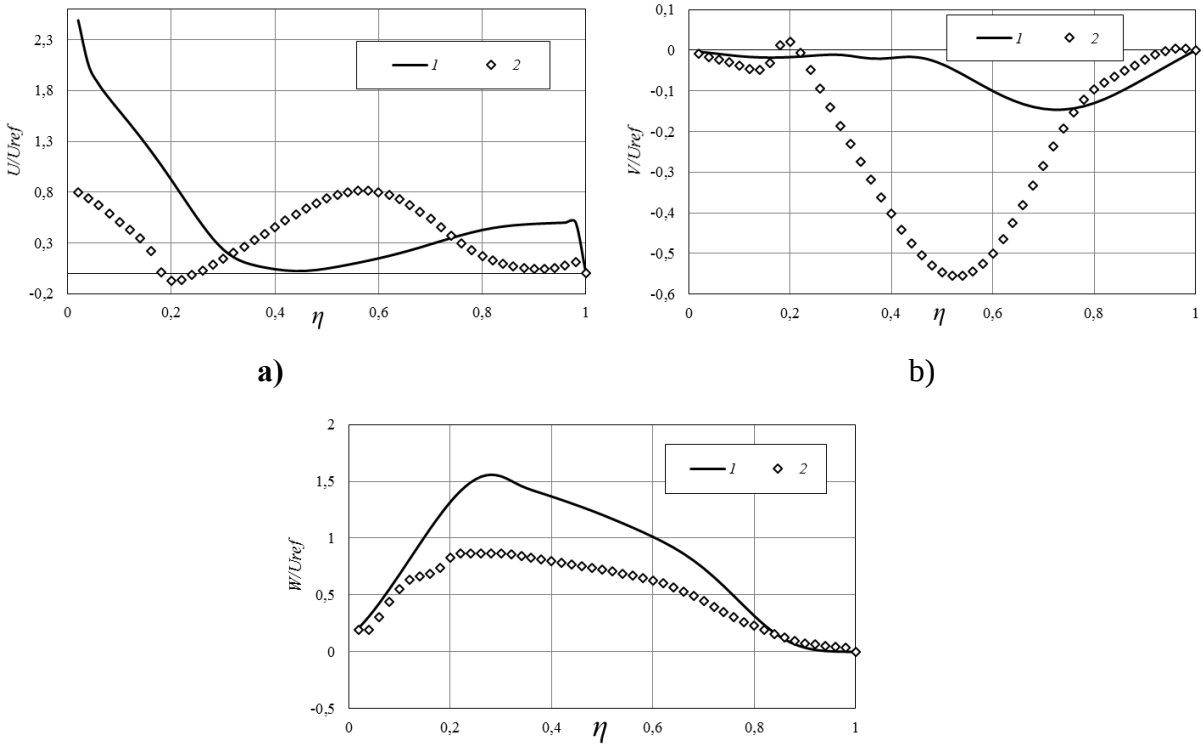

a) b)

c)

Fig.3. Profiles of a) axial, b) radial and c) tangential air flow velocities in the section ξ=0.65 at $Wref/Uref$=1. 1- using vorticity and stream function, 2- Semi-implicit method for pressure-binding SIMPLE.

On fig. 4 illustrates the profiles of air velocities in the section $\xi = 0.7$. Here $U/Uref, V/Vref, W/Wref$ - dimensionless speeds. Here $Uref = U_0, Wref/Uref = 1$.

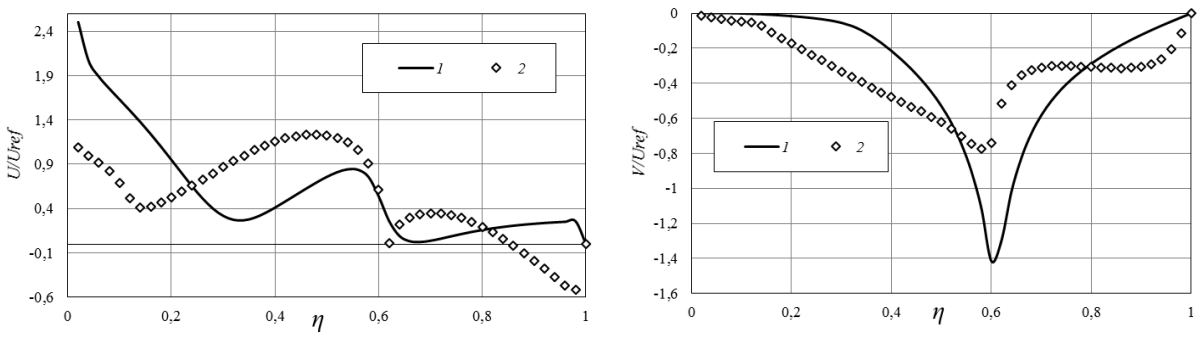

a) **b)**

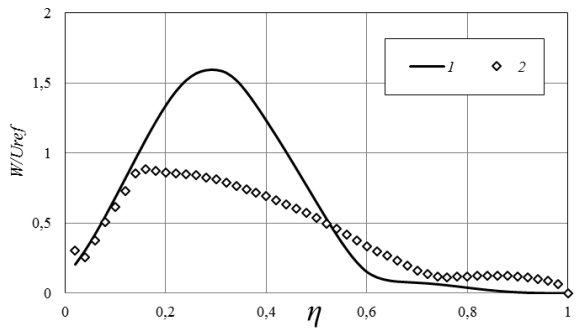

c)

Fig.4. Profiles of a) axial, b) radial and c) tangential air flow velocities in the section ξ=0.7 at *Wref* /*Uref* =1. 1- using vorticity and stream function, 2- Semi-implicit method for pressure-binding SIMPLE.

On Fig. 5. The vector velocity field in the central section is shown.

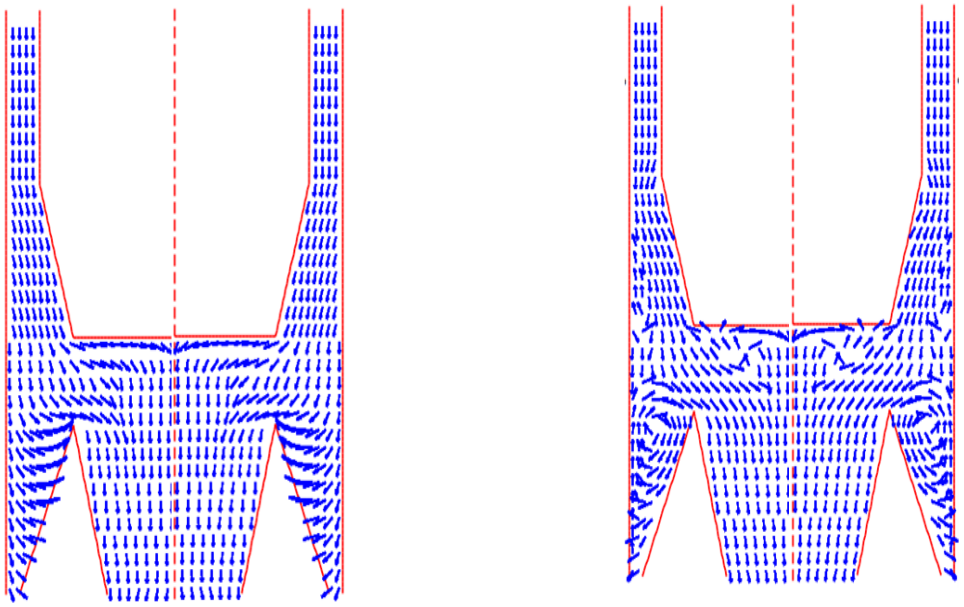

a) **b)**

Fig. 5. a- Using vorticity and stream function, b- Semi-implicit method for pressure-binding SIMPLE.

FINDINGS

It can be seen from the presented figures that the numerical results of the SA and SARC models differ quite significantly. However, it is noted in [2, 4] that for swirling flows the SARC model gives results that are closer to the experimental data. Therefore, it can be assumed that the SARC turbulent model is more suitable for describing the processes occurring inside centrifugal apparatuses.

BIBLIOGRAPHY

1. Гупта А., Лили Д., Сайред Н. Закрученные потоки. — М.: Мир, 1987. — 590 с.
2. Muntean S., Susan-Resiga R. F., Bosioc A. I. Proc. 3th IAHR International Meeting of the Workgroup on Cavitation and Dynamic Problems in Hydraulic Machinary and Systems, October 14–16, 2009, Brno, Czech Republic.

3. Okulov V. L., Sorensen J. N. Maximum efficiency of wind turbine rotors using Joukowsky and Betz approaches. Journal of Fluid Mechanics. — 2010. — Vol. 649. — P. 497–508.
4. Syred N. A review of oscillation mechanisms and the role of the precessing vortex core (PVC) in swirl combustion systems // Prog. Energy Combust. Sc. — 2006. — Vol. 32 (2). — P. 93–161.
5. Derksen J. J. Separation performance predictions of a Stairmand high-efficiency cyclone // AIChEJ.—2003. — Vol. 49, no. 6. — P. 1359–1371.
6. Spalart P.R., Allmaras S.R. A one-equation turbulence model for aerodynamic flow // AIAA Paper. – 1992.–12;1. – P.439–478.
7. Лойцянский Л.Г. Механика жидкости и газа /Л.Г.Лойцянский. – М.: Наука. 1987–840с.
8. Bradshaw P., Ferriss D. H., Atwell N. P. “Calculation of boundary layer development using the turbulent energy equation”, J. Fluid Mech., 1967. 28, c.593-616
9. Mises R., Zs. angew. Math. u. Mech., 7, 1927. c. 425.
10. Patankar S.V. Numerical Heat Transfer and Fluid Flow. Taylor&Francis. ISBN 978-0-89116-522-4, 1980.
11. Launder B.E., Spalding D.B. Lectures in Mathematical Models of Turbulence. - London: Academic Press, 1972. - 169 p.
12. Malikov Z. M., Madaliev E. U. Mathematical simulation of the speeds of ideally newtonovsky, incompressible, viscous liquid on a curvilinearly smoothed pipe site //Scientific-technical journal. – 2019. – T. 22. – №. 3. – C. 64-73.
13. Malikov Z. M., Madaliev E. U., Madaliev M. E. Numerical modeling of a turbulent flow in a flow flat plate with a zero gradient of pressure based on a standard k-ε and modernized k-ε models //Scientific-technical journal. – 2019. – T. 23. – №. 2. – C. 63-67.
14. Abdukarimov, B. A., & Kuchkarov, A. A. (2022). Research of the Hydraulic Resistance Coefficient of Sunny Air Heaters with Bent Pipes During Turbulent Air Flow. Journal of Siberian Federal University. Engineering & Technologies, 15(1), 14-23.
15. Abdukarimov, B. A. (2021). Improve Performance Efficiency As A Result Of Heat Loss Reduction In Solar Air Heater. International Journal of Progressive Sciences and Technologies, 29(1), 505-511.
16. Malikov, Z. M., & Madaliev, M. E. (2020). Numerical simulation of two-phase flow in a centrifugal separator. Fluid Dynamics, 55(8), 1012-1028.
17. Маликов, З. М., & Мадалиев, М. Э. (2021). Численное моделирование течения в плоском внезапно расширяющемся канале на основе новой двужидкостной модели турбулентности. Вестник Московского государственного технического университета им. НЭ Баумана. Серия «Естественные науки», (4 (97)), 24-39.
18. Madraximov, M. M., Abdulkhaev, Z. E., & ugli Inomjonov, I. I. (2022). Factors Influencing Changes In The Groundwater Level In Fergana. International Journal of Progressive Sciences and Technologies, 30(2), 523-526.
19. Arifjanov, A., Otaxonov, M., & Abdulkhaev, Z. (2021). Model of groundwater level control using horizontal drainage. Irrigation and Melioration, 2021(4), 21-26.
20. Худайкулов, С. И., & Муминов, О. А. У. (2022). МОДЕЛИРОВАНИЯ МАКСИМАЛЬНОЙ СКОРОСТИ ПОТОКА ВЫЗЫВАЮЩЕЙ КАВИТАЦИЮ И

РЕЗКОЙ ПЕРЕСТРОЙКИ ПОТОКА. Universum: технические науки, (2-2 (95)), 59-64.

21. АБДУЛҲАЕВ, З., & МАДРАХИМОВ, М. (2020). Гидротурбиналар ва Насосларда Кавитация Ҳодисаси, Оқибатлари ва Уларни Бартараф Этиш Усуллари. Ўзбекгидроэнергетика" илмий-техник журнали, 4(8), 19-20.
22. ugli Mo'minov, O. A., Maqsudov, R. I., & qizi Abdukhalilova, S. B. (2021). Analysis of Convective Finns to Increase the Efficiency of Radiators used in Heating Systems. Middle European Scientific Bulletin, 18, 84-89.
23. Усмонова, Н. А., Негматуллоев, З. Т., Нишонов, Ф. Х., & Усмонов, А. А. (2019). Модели закрученных потоков в строительстве Каркидонского водохранилища. Достижения науки и образования, (12 (53)), 5-9.
24. Абдукаримов, Б. А., Аббасов, Ё. С., & Усмонова, Н. У. (2019). Исследование рабочих параметров солнечных воздухонагревателей способы повышения их эффективности. Матрица научного познания, (2), 37-42.
25. Мадрахимов, М. М., & Абдулҳаев, З. Э. (2019). Насос агрегатини ишга туширишда босимли сув узатгичлардаги ўтиш жараёнларини ҳисоблаш усуллари. Фарғона Политехника Институти Илмий–Техника Журнали, 23(3), 56-60.
26. Mamadalievich, M. M., & Erkinjonovich, A. Z. Principles of Operation and Account of Hydraulic Taran. JournalNX, 1-4.
27. Сатторов, А. Х. (2016). СУЩЕСТВОВАНИЕ И ПРЕДСТАВЛЕНИЕ ОГРАНИЧЕННОГО РЕШЕНИЯ ОДНОГО КВАЗИЛИНЕЙНОГОДИФФЕРЕНЦИАЛЬНОГО УРАВНЕНИЯ. In Вузовская наука-региону (pp. 126-132).
28. Мадхадимов, М. М., Абдулхаев, З. Э., & Сатторов, А. Х. (2018). Регулирования работы центробежных насосов с изменением частота вращения. Актуальные научные исследования в современном мире, (12-1), 83-88.
29. Abdikarimov, R., Usarov, D., Khamidov, S., Koraboshev, O., Nasirov, I., & Nosirov, A. (2020, July). Free oscillations of three-layered plates. In IOP Conference Series: Materials Science and Engineering (Vol. 883, No. 1, p. 012058). IOP Publishing.
30. Nosirov, A. A., & Nasirov, I. A. (2021). Natural and Forced Vibrations of Axisymmetric Structure Taking into Account the Viscoelastic Properties of the Base. Middle European Scientific Bulletin, 18, 303-311.
31. qizi Abdukhalilova, S. B. (2021). Simplified Calculation of the Number of Bimetallic Radiator Sections. CENTRAL ASIAN JOURNAL OF THEORETICAL & APPLIED SCIENCES, 2(12), 232-237.
32. Maqsudov, R. I., & qizi Abdukhalilova, S. B. (2021). Improving Support for the Process of the Thermal Convection Process by Installing. Middle European Scientific Bulletin, 18, 56-59.
33. Мадрахимов, М. М., Абдулҳаев, З. Э., & Ташпулатов, Н. Э. (2019). Фарғона Шаҳар Ер Ости Сизот Сувлари Сатҳини Пасайтириш. Фарғона Политехника Институти Илмий–Техника Журнали, 23(1), 54-58.
34. Hamdamov, M., Mirzoyev, A., Buriev, E., & Tashpulatov, N. (2021). Simulation of non-isothermal free turbulent gas jets in the process of energy exchange. In E3S Web of Conferences (Vol. 264, p. 01017). EDP Sciences.
35. Рашидов, Ю. К., Орзиматов, Ж. Т., & Исмоилов, М. М. (2019). Воздушные

солнечные коллекторы: перспективы применения в условиях Узбекистана. In Экологическая, промышленная и энергетическая безопасность-2019 (pp. 1388-1390)

36. Рашидов, Ю. К., Исмоилов, М. М., Орзиматов, Ж. Т., Рашидов, К. Ю., & Каршиев, Ш. Ш. (2019). Повышение эффективности плоских солнечных коллекторов в системах теплоснабжения путём оптимизации их режимных параметров. In Экологическая, промышленная и энергетическая безопасность-2019 (pp. 1366-1371).
37. Madraximov, M. M., Abdulkhaev, Z. E., & Orzimatov, J. T. (2021). GIDRAVLIK TARAN QURILMASINING GIDRAVLIK HISOBI. Scientific progress, 2(7), 377-383.
38. Rashidov, Y. K., & Orzimatov, J. T. (2022). SOLAR AIR HEATER WITH BREATHABLE MATRIX ABSORBER MADE OF METAL WIRE TANGLE. Scientific-technical journal, 5(1), 7-13.
39. Усаров, М. К., & Маматисаев, Г. И. (2019). КОЛЕБАНИЯ КОРОБЧАТОЙ КОНСТРУКЦИИ КРУПНОПАНЕЛЬНЫХ ЗДАНИЙ ПРИ ДИНАМИЧЕСКИХ ВОЗДЕЙСТВИЯХ. In Научный форум: технические и физико-математические науки (pp. 53-62).
40. Abdukarimov, B., O'tbosarov, S., & Abdurazakov, A. (2021). Investigation of the use of new solar air heaters for drying agricultural products. In E3S Web of Conferences (Vol. 264, p. 01031). EDP Sciences.
41. Усаров, М. К., & Маматисаев, Г. И. (2014). К динамическому расчету коробчатой конструкции здания. ME′ MORCHILIK va QURILISH MUAMMOLARI, 86.
42. Bekzod, A. (2020). Relevance of use of solar energy and optimization of operating parameters of new solar heaters for effective use of solar energy. IJAR, 6(6), 16-20.
43. Madraximov, M. M., Nurmuxammad, X., & Abdulkhaev, Z. E. (2021, November). Hydraulic Calculation Of Jet Pump Performance Improvement. In International Conference On Multidisciplinary Research And Innovative Technologies (Vol. 2, pp. 20-24).
44. Hamdamalievich, S. A., & Nurmuhammad, H. (2021). Analysis of Heat Transfer of Solar Water Collectors. Middle European Scientific Bulletin, 18, 60-65.
45. Madaliev, M. E. U., Maksudov, R. I., Mullaev, I. I., Abdullaev, B. K., & Haidarov, A. R. (2021). Investigation of the Influence of the Computational Grid for Turbulent Flow. Middle European Scientific Bulletin, 18, 111-118.
46. Madraximov, M., Yunusaliev, E., Abdulhayev, Z., & Akramov, A. (2021). Suyuqlik va gaz mexanikasi fanidan masalalar to'plami. GlobeEdit.
47. Абдукаримов, Б. А., Акрамов, А. А. У., & Абдухалилова, Ш. Б. К. (2019). Исследование повышения коэффициента полезного действия солнечных воздухонагревателей. Достижения науки и образования, (2 (43)).
48. Умурзакова, М. А., Усмонов, М. А., & Рахимов, М. Н. (2021). АНАЛОГИЯ РЕЙНОЛЬДСА ПРИ ТЕЧЕНИЯХ В ДИФФУЗОРНО-КОНФУЗОРНЫХ КАНАЛАХ. Экономика и социум, (3-2), 479-486.
49. Аббасов, Ё. С., & Умурзакова, М. А. (2020). РАСЧЕТ ЭФФЕКТИВНОСТИ ПЛОСКИХ СОЛНЕЧНЫХ ВОЗДУХОНАГРЕВАТЕЛЕЙ. In Современные проблемы теплофизики и энергетики (pp. 7-8).